

Multiband L5 capable GPS antenna

Yoonjae Lee and Suman Ganguly, *Center for Remote Sensing, Inc.*
Raj Mittra, *Electromagnetic Communication Laboratory, Pennsylvania State University*

BIOGRAPHY

Yoonjae Lee is a research engineer at Center for Remote Sensing, Inc. He received B.S. degree in Electronic Communication Engineering from Kwangwoon University, Seoul, Korea and M.S. degree in Electrical Engineering from the Pennsylvania State University (Penn State). He specializes in design, simulation, modeling and software development for electromagnetic problems in various applications including antenna, microwave, electromagnetic scattering and radiation and EMI/EMC using Method of Moment (MoM), Finite Difference Time Domain (FDTD), Finite Element Method (FEM), and other numerical techniques.

Suman Ganguly has been working in the areas of radio science, radio engineering, electronics, ionospheric and plasma physics for over 30 years. He graduated from Calcutta University, India with a Masters in physics and electronics in 1962 and a Ph.D. in 1970. Since then, he has been working in a variety of disciplines and in different institutions. During 1986, he started a small R&D organization, Center for Remote Sensing, in Virginia and has been active in numerous projects involving communication, navigation, signal processing and other areas of radio engineering. He has directed more than 50 projects supported under various segments of DoD, NASA, and NSF. He has over 100 publications and is a member of numerous professional organizations.

Raj Mittra is a Professor in the EE department at the Pennsylvania State University. He obtained his Ph.D. in Electrical Engineering from University of Toronto in 1957. He has been with the University of Illinois, Oxford University in England and the Technical University in Denmark. He has published more than twenty-five books or book chapters, and over 680 papers in refereed journals in the areas of antennas, computational electromagnetics, microwaves, and related fields. He is a Life Fellow of the IEEE. He has been awarded the IEEE Centennial medal and a Guggenheim fellowship. He holds one patent in the

area of Communication antenna design and has another patent pending. He has served as a consultant to many government and industrial organization.

ABSTRACT

We present a novel multiband antenna design for GPS applications at three (L_1 - 1575.42MHz, L_2 - 1227.60MHz and L_5 - 1176.45MHz) different frequencies using the aperture coupled stacked patch configuration. The multi-frequency operation is quite demanding in various GPS applications, for instance, L_1 and L_2 data is required for differential GPS applications and the future GPS will be using additional L_5 band. For such applications, it is desirable to use a single antenna for multi-frequency. The designed antenna is capable of operating at three different bands with improved performances in terms of bandwidth, axial ratio, cross-pol rejection level and multipath rejection characteristic. To mitigate the multipath interference, we use a novel structure, in which multiple conducting plates combined with conducting cylinders in between, that suppresses the diffraction from the ground plane edges and effectively suppress the back lobe without increasing the diameter of the ground plane. Finite Element (FEM) electromagnetic modeling has been performed for designing the antenna. The designed antenna has been fabricated and tested.

INTRODUCTION

In 1999, the US announced a GPS modernization initiative, a part of which is the availability of a second civil signal on the existing L_2 frequency and a third civil signal on the new L_5 frequency [1]. The L_5 signal will be transmitted by the Block IIF satellites, the first of which will be available in 2005. The 24MHz bandwidth extension for the current L_1 and L_2 signal is also proposed to carry the new military M-code.

This paper describes a new antenna for the recent development of the GPS technology. The new antenna

will cover the new L_3 band as well as the current L_1 and L_2 bands with increased bandwidths and superior multipath rejection to support the future system. Recently, several GPS antenna designs with improved multipath rejection capabilities and reduced sizes for high precision survey have been appeared. Considerable efforts have also been made in the past to utilize Electromagnetic Bandgap (EBG) structures for antenna pattern control [2]. However, there have been some drawbacks such as large ground plane size, high vertical profile, insufficient F/B ratio and pattern roll-off. The new antenna uses a stacked patch configuration for increased bandwidth and aperture coupled feeding structure to ease the matching problems and the fabrication of complicated feeding network for circular polarization at multiple frequency. The superior F/B ratio and pattern roll-off characteristic is achieved by using a novel back lobe suppressor (vertical choke ring), which enables to suppress back lobes as effectively as the conventional choke ring with greatly reduced size (diameter = 180mm, height = 40mm). Extensive numerical simulations have been performed to obtain the optimum performances. The prototype antenna has been fabricated and tested.

CIRCULARLY POLARIZED APERTURE COUPLED STACKED PATCH ANTENNA

Circularly polarized multiband microstrip antennas can be made using various structures and feeding schemes. Slot loaded patches [3] are widely used and phased array configurations of multiband antennas, such as fractal [4], are also possible. An alternative would be to use a combined antenna element for multiband coverage [5].

The most commonly used feeding methods for microstrip patch antennas are coaxial probe, stripline directly connected to a patch and stripline coupled to the patch through an aperture. The advantage of directly connected stripline is ease of fabrication. However, there are disadvantages such as inconvenient impedance matching compared to the probe case and unwanted radiation from the feed lines. The aperture coupled microstrip patch antenna [6] has become very popular in which the energy from the stripline is coupled to the patch element through an aperture (slot) in the ground plane. Some of advantages of the aperture coupled microstrip antenna are: (a) the feed network is isolated from the radiating element; (b) active devices can be fabricated in a feed substrate for which the dielectric constant can be chosen independently to the substrates for the patches; (c) increased impedance bandwidth is achieved; (d) the design can be more robust. The impedance bandwidth of an aperture coupled patch antenna is typically 6-7 percent, whereas that of a coaxially fed microstrip patch antenna is approximately 2-3 percent.

The vertical layout of the designed antenna is shown in Fig. 1. The antenna consists of two stacked circular patches and they are excited through four apertures in the ground plane. The four apertures (slots) provide 90-degree phase shift at each slot location to achieve the circular polarization. The top patch resonates at L_1 band (1575.42MHz) and the bottom patch resonates at the center of L_2 (1227.6 MHz) and L_3 (1176.45MHz) band. The required bandwidth for each band is 20MHz. Since the aperture coupled stacked patch antenna has wider impedance matching characteristic and axial ratio bandwidth, we attempted to cover the two lower bands (L_2 and L_3) with a single patch with the aid of stacked L_1 patch as a parasitic element at lower frequency bands. The patches are coupled through slots to the feeding microstrip lines in the backside of the bottom substrate. The slot locations and dimensions must be optimized for the good matching characteristic with the patch and feed network as well as required axial ratio and cross-pol rejection level. The feed line is designed to provide a good phase offsets and minimal phase errors for each exciting slots.

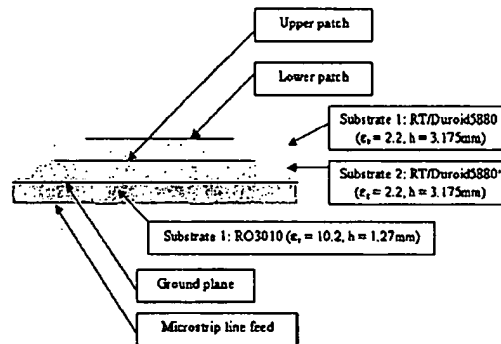


Figure 1. Circularly polarized aperture coupled stacked patch antenna

DESIGN PROCEDURE

The design procedure for the aperture-coupled stacked patch antenna should be taken properly because all the design parameters are interrelated and must be optimized altogether. We summarize the design procedure that yields parameters close to optimum. The design parameters to be determined are patch sizes, aperture dimension and location and substrate properties (height, dielectric constant, and etc.) associated with the layouts shown in Fig 1. The first step of the design is to determine the patch sizes for each band. When the substrate height is very small ($h \ll 0.05\lambda$), the resonant frequency of the microstrip antenna is well approximated by the cavity model [7]. We use thick low permittivity substrate for the patch to obtain the maximum bandwidth. Dielectric constant 2.2 is widely used and the board material is readily available. The substrate height has been chosen to

be 3.175mm. The resonant frequencies for the TM_{mn}^2 of the circular patch antenna are found to be

$$(f_r)_{mn0} = \frac{1}{2\pi\sqrt{\mu\epsilon}} \left(\frac{\chi'_{mn}}{a} \right) \quad (1)$$

where χ'_{mn} is the zeros of the derivative of the Bessel function $J_m(x)$ and a is the radius of the circular patch. The patch radius for the dominant mode is given by

$$a = \frac{1.8412}{2\pi f \sqrt{\epsilon_r}} \quad (2)$$

where c is the speed of light in free space. However, this resonant frequency of (2) does not take into account fringing effect which makes the patch look electrically larger. This may be corrected by using the correction factor and the resulting relation is given by [8]

$$a_e = a \left\{ 1 + \frac{2h}{\pi\epsilon_r} \left[\ln \left(\frac{\pi a}{2h} \right) + 1.7726 \right] \right\}^{1/2} \quad (3)$$

The two design frequencies are 1575.42MHz and 1201MHz (center frequency of the L_2 and L_3) and the calculated corresponding patch radii are 35.63mm and 47.22mm, respectively. The patch dimensions calculated by (3) are used for the initial designs and later optimized. The resonant sizes of the patches must be determined simultaneously due to the coupling between the patches.

The design of the optimum slot dimension and location is not an easy task because there are no general design formulas available. The effect of the slot dimensions to the antenna is dependent to the antenna geometry, in general. Larger slot length introduces the higher coupling between the patch and feed line, but that also shifts the resonant frequencies and increases the unwanted back radiation. The location of the slot affects the resonant frequency, cross-pol pattern and the impedance matching between the feed line and patches. Now it is evident that determining the parameters one by one is impossible for large number of strongly coupled parameters. For this type of design, the design strategy would be to reduce the number of design parameters by pre-selecting some fixed design choices and optimize the initial design using the numerical modeling tools. The initial patch sizes are determined by (3) and the bottom substrate height and dielectric constant is chosen after finding the slot locations and dimensions because there are some design flexibilities for the feed lines depending upon how to choose the substrate parameters. The slots in the aperture coupled antenna are considered as a series reactance between the patch and feed line and that effect can be

eliminated by placing additional open circuited stub after the slot. Once the slot parameters are chosen, then the feed line is designed for circular polarization. There are four 90 degree rotated slots each incorporated in the ground plane and lower patch. At lower band, the most of the energy is coupled to the lower patch and the upper patch is parasitically coupled to the lower patch, which provides required additional bandwidth for the lower band (1164.45MHz – 1239.60MHz, 24MHz BW considered for each band for future extension) and at upper band, the lower patch is more tightly coupled to the ground plane, so the lower patch effectively acts like a ground plane to the upper patch.

The initial slot dimensions and locations have been found for the single slot, single feed, linearly polarized circular patch antenna and the effect of the variation has been studied, then applied to the circularly polarized antenna. The feed line is a leaky microstrip line designed to be matched to 50- Ω output impedance. 90-degree phase offset has been achieved using quarterwave stripline. An important design goal is that the feed line must maintain minimal phase error and impedance variations over the entire band (L_3 through L_1). We design the feed line for the center frequency (1.4GHz) of the three bands and use a relatively high permittivity substrate to restrain the impedance variations and phase errors introduced by changes of the electrical length of the feed line as the operating frequency has offset to the center frequency since the required correction for the physical dimensions of the feed lines on the high permittivity substrate is less than that is required for the low permittivity substrate for the same frequency offset.

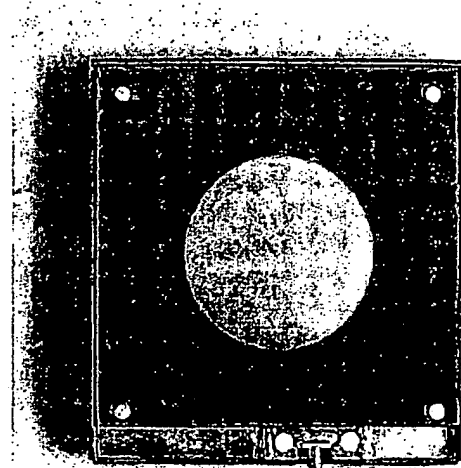


Figure 2. Tri-band GPS antenna prototype

The final design has been obtained by iterating the above steps within a fixed range of variation for the each parameter. The fabricated prototype antenna is shown in Fig. 2.

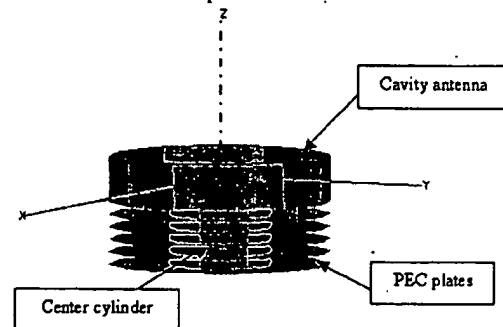
VERTICAL CHOKE RING

Multipath is a limiting factor in precision GPS applications. Multipath signals are coming in with arbitrary incident angles to the antenna depending upon the environment around the antenna. However, the multipath signals from below horizon due to the reflections from the ground and mounting structure are main concerns because the antenna is usually mounted less than 2 meters above the ground and it is difficult for the signal processing in the receiver to mitigate the effect of short distance multipath (less than 10 meters). In this case, the multipath signals can be suppressed by tailoring the receiving pattern of the antenna. The ideal GPS antenna would be one that has a uniform gain for the upper hemisphere and blocks the signal coming from below the horizon. JPL conducted extensive experimental investigations on several different ground plane structures including circular metallic sheets, absorbers and choke rings and concluded that the corrugated surface structures showed the most promising pattern roll-off and back lobe levels. Later, a theoretical model of the corrugated ground plane was developed later by Tranquilla [9].

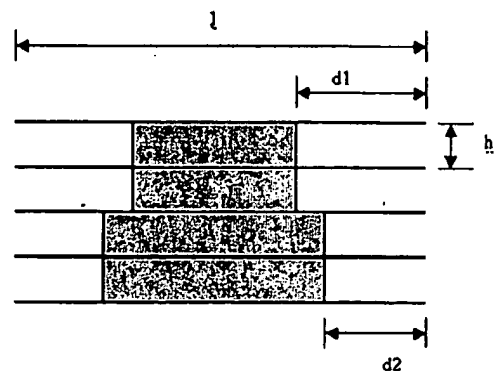
The conventional choke ring ground plane consists of several concentric thin metallic rings around the antenna element and the bottom of the ring is connected to a thick conducting circular disk. If the height of the wall (ring) is chosen to be close to quarter wavelength of the operating frequency, the top end of the rings can be effectively made to be an open circuit, in which the wave propagation to the direction of horizon is suppressed. Because of the ring depth has to be determined by the operating frequency, the choke ring has optimum effect only on the particular frequency. Recently, an attempt has been made to realize a dual frequency choke ring [10]. The concept was to use a special diaphragm (slot filter) inside the choke ring groove that blocks the high frequency but passes lower frequencies, so that the groove depth could be made different for two frequencies. One of the drawbacks of the conventional choke ring is that it has fairly large footprints (typically 15"). Realization of a reduced size antenna with comparable performances to the standard choke ring antenna is particularly demanding.

We present a new design concept of the choke ring, which greatly reduces the overall size, but still maintains the capabilities of suppressing the back lobe and enhancing the pattern roll-off characteristic comparable to the standard choke ring. Fig. 3 shows the new design of choke ring. The new design uses multiple conducting

circular plates instead of using ring type walls. The grooves are made by adjacent plates and center cylinders. They can be vertically stacked to increase the effect of suppression. The depth of the groove is determined by wavelength of the intended frequency. The concept has been investigated by numerical simulations and experimentally proved. The simulated model is shown in Fig. 3 (a). The antenna element chosen for the simulation is a cavity backed cross dipole resonating at 1.1GHz and the new vertical choke ring consists of five stacked grooves, which are attached to the bottom of the cavity. The diameter of the cavity and vertical choke ring is 180mm and the overall height of the vertical choke ring is 50mm, which are much smaller dimensions compared to those of the conventional choke rings. The groove depth has been varied to find an optimum choice. The Front/Back ratio vs. groove depth is shown in Table 1. The optimum depth has been found to be 0.18λ for the given configuration, which is somewhat less than the quarterwave length of the operating frequency. Our research shows that the optimum depth varies depending upon the diameter of the choke ring and the separation distance of the circular plates.



a. cavity antenna with single frequency vertical choke ring



b. vertical profile of the dual-frequency vertical choke ring

Figure 3. Vertical choke ring

The Ansoft-HFSS[®] [11] has been used to simulate the antenna and vertical choke ring and the results are shown in Fig. 4. In Fig. 4, the total field patterns (RHCP+LHCP) are compared for antenna only, 400mm standard choke ring, 240mm choke ring, and 180mm vertical choke ring. We can see from Fig. 4 that the 180mm vertical choke ring suppresses the back lobe level by approximately 10 dB, which is the same performance of the 240mm choke ring ground plane. Next, we investigated the back lobe suppression levels versus number of groove. The number of groove varied from 0 to 6 and the corresponding F/B ratios have been plotted in Fig. 5. It is observed that the enhancement of F/B ratio is most noticeable up to three grooves and after that, the degree of enhancement decreases. Fig. 6 shows the effect of groove width (h). As shown in the figure, a wider groove has suppression effect over a wider frequency range. We also note that the suppression levels rapidly fall off toward the lower frequency than upper frequency.

Radius of the PEC plates (mm)	Depth (mm)	Depth (wavelength @ 1.1GHz)	Front/Back ratio (dB)
Antenna Only			16
90	68.25	0.25	21
90	65	0.24	22
90	60	0.22	20
90	55	0.20	23
90	50	0.18	27.5
90	45	0.165	24

Table 1. Front/Back ratio vs. choke ring depth for the 5-groove vertical choke ring

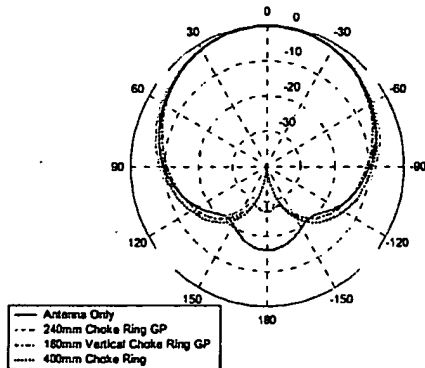


Figure 4. Comparison of the simulated directivity patterns for different ground plane configurations

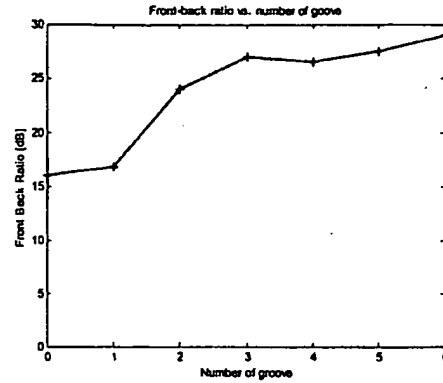


Figure 5. Front/Back ratio vs. number of groove

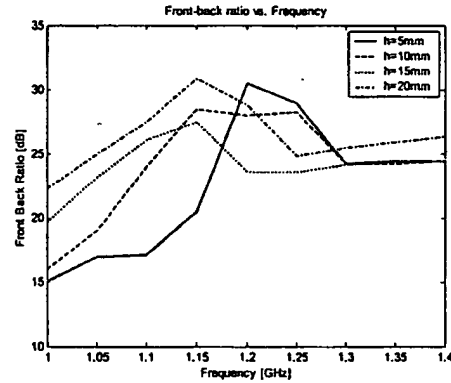


Figure 6. Front/Back ratio vs. frequency for different groove width (h)

The choke ring shown in Fig. 3 (a) is only effective for a single frequency. In order to make the vertical choke ring operate for three frequencies (L_1 , L_2 and L_3), we stack vertical choke rings with different groove depths as shown in Fig. 3 (b). The operating bandwidth of the vertical choke ring is wide enough to cover the L_2 and L_3 band simultaneously, we chose the center frequency of the lower band choke ring depth (d_1) to be the center frequency of L_2 (1227.60MHz) and L_3 (1176.45MHz). The choke ring width (h) has been chosen to be 10 mm because the bandwidth and suppression levels do not significantly increase by increasing the choke ring width (h), which eventually results in the increased overall dimensions. The designed vertical choke ring for the tri-band GPS antenna has four center cylinders and five circular disks, in which upper two grooves are designated for L_2/L_3 and lower ones are for L_1 . Using two grooves for each band is most size-effective considering the overall footprint of the structure. The overall height of the vertical choke ring for tri-band GPS antenna is 40mm and the diameter is 180mm, which are much smaller than

those of the standard choke ring (height $\approx 65\text{mm}$, diameter $= 350\text{--}400\text{mm}$). The tri-band GPS antenna with vertical choke ring is shown in Fig. 7. Increasing the number of grooves further improves the suppression level, but the amount of improvement is insignificant while overall dimension significantly increases.

EXPERIMENTAL RESULTS AND COMPARISON STUDY

The designed antenna has been fabricated on the Rogers[®] dielectric substrates. RT/Duroid[®] 5880 ($\epsilon_r=2.2$, $h=3.175\text{mm}$) is used for the two circular patches (substrates 1 and 2) and RO3010 ($\epsilon_r=10.2$, $h=1.27\text{mm}$) is used for the ground plane and microstrip feed lines (substrate-3). The patches, apertures and feeding microstrip lines are chemically etched. The feeding microstrip line is printed on the backside of the substrate-3 and connected to an SMA connector. In order to prevent unwanted radiation from the feeding network, the backside of the antenna has been encapsulated by using the ECCOSORB[®] FGM-40 microwave absorbing material and additional conducting sheet has been placed at the bottom surface of the antenna. The four sides of the antenna are shield by only the absorbing material so that the surface waves on the antenna can be absorbed. The side shielding of the antenna by additional copper sheet outside surface of the absorber introduces more back radiation.

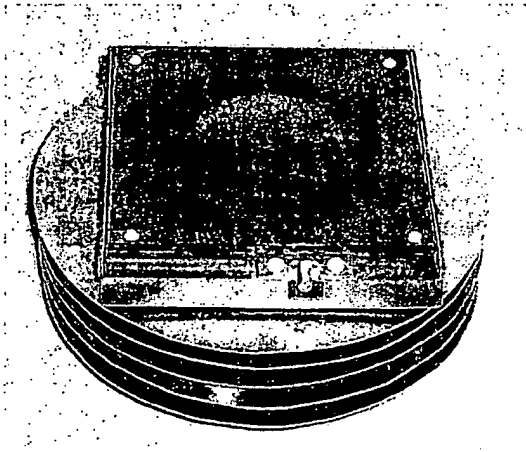


Figure 7. Vertical choker ring with the tri-band GPS antenna

The fabricated antenna is shown in Fig. 2 and dimensions are $140\text{mm(L)} \times 140\text{mm(W)} \times 17.6\text{mm(H)}$. The return loss characteristic of the fabricated antenna has been measured using HP-8510 network analyzer and the result is shown in Fig. 8. As shown in the plot, the designed antenna has very wide matching characteristics over the

GPS bands. The antenna pattern measurement has been performed in the anechoic chamber. Figures 9, 10 and 11 show the RHCP and LHCP patterns of the designed antenna without vertical choke ring. The cross-polarization levels for three operating bands are approximately -20 dB at boresight, which are desirable. The back lobe levels of RHCP patterns are close to -30 dB for all operating frequencies. For a comparison study, the Pinwheel[™] antenna [12] has been also measured and patterns are plotted in Figs. 12 and 13. The designed tri-band antenna shows comparable cross-pol levels with the Pinwheel[™] antenna. The Pinwheel[™] antenna has cardioid RHCP patterns for both operating frequencies, but its LHCP patterns have significant back lobes. In general, the reflected multipath signals can be either left-hand or right-hand polarized with arbitrary axial ratios depending upon the number of reflections and the material properties of the reflecting media. The multipath signals from the upper hemisphere result from the surrounding environment such as buildings and terrains, which are also arbitrarily polarized. However, the strongest multipath signals from the upper hemisphere are the signals that have been reflected one time and they are mitigated by cross-pol (LHCP) suppression of the antenna. The multipath signals from upper hemisphere are relatively long-distance multipath signals that also can be mitigated by signal processing of the received signals while on the other hand the multipath signals coming from below the horizon are, in general, strong left hand polarized waves reflected from the ground. These multipath signals are difficult to be mitigated unless the antenna has excellent roll-off for both left-hand and right-hand polarizations for the lower hemisphere. We point out that a good multipath resilient antenna must have minimum back lobes for both polarizations.

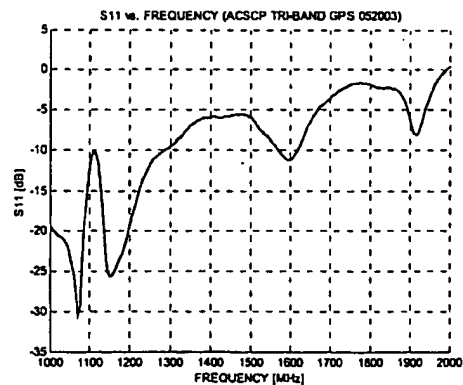


Figure 8. S11 ($Z_0=50\Omega$) of the tri-band GPS antenna

The total field patterns (LHCP+RHCP) of the tri-band GPS antenna have been measured at three operating frequencies, which are 1176.45MHz , 1227.6MHz , and

1575.42MHz, respectively. The measured results are compared with the Pinwheel™ antenna. The measured Front/Back ratios are shown in Table. 2. From Figs. 14 through 16, we note that the back lobe levels are greatly reduced and roll-off characteristic is improved by using vertical choke ring at all three operating frequencies. The tri-band antenna with vertical choke ring has similar roll-off characteristic with the Pinwheel™ antenna but the back lobe levels of the tri-band antenna for $140 < \theta < 180$ are lower than that of the Pinwheel™ antenna both at L_1 and L_2 frequencies (see Figs 14 and 15). Figs 17 and 18 show the comparison of the up/down gain ratio for the tri-band antenna and the Pinwheel™ antenna. At L_1 band, the Pinwheel™ antenna shows flat 20 dB up/down gain ratio up to $\theta=60^\circ$ and 0.6dB/deg roll-off after that. The tri-band GPS antenna without vertical choke ring shows higher up/down gain ratio only up to $\theta=30^\circ$ and 0.3dB/deg roll-off for $\theta > 30^\circ$. However, it is shown that the vertical choke ring greatly increases the up/down gain ratio and the roll-off becomes comparable to the Pinwheel™ antenna and for $0^\circ < \theta < 40^\circ$, the tri-band antenna shows higher up/down gain ratio than the Pinwheel™ antenna. The tri-band GPS antenna exhibits comparable results with the Pinwheel™ antenna at L_1 band even without the vertical choke ring, and with the choke ring the up/down gain ratio is enhanced by 5 dB for $\theta < 40^\circ$. The results at the L_1 band are shown in Fig. 20. The roll-off improvement by vertical choke ring is also obvious here.

CONCLUSION

We have shown a promising new antenna design for precision survey GPS applications. The designed antenna covers two existing GPS bands (L_1/L_2) as well as the new L_5 band. The antenna is compatible with the future system in which the bandwidth requirement is 20 percent increased. The antenna offers a good circular polarization and a uniform hemispherical gain pattern for three operating bands. The vertical choke ring ground plane provides excellent below-horizon multipath suppression for all of its operating bands. The antenna can be easily fabricated using the microstrip line structure. The overall size of the antenna is 140 mm in length and width, which is very practical to be adopted in the mounting platform for various applications.

ACKNOWLEDGMENTS

This work was partially supported through the SBIR contract (No. F33615-01-C-1873) for Wright Patterson AFB, OH. The authors thank Joseph Tenbarger for his advice and support.

REFERENCES

- [1] "GPS Modernization",

<http://ntiacsd.ntia.doc.gov/gps/gpsmodern.html>

- [2] Y. Lee, J. Yeo and R. Mittra, "Investigation of electromagnetic bandgap (EBG) structures for antenna pattern control," *IEEE Antennas and Propagation Society International Symposium*, Vol. 2, pp. 1115–1118, June, 2003.

- [3] F. Yang and Y. Rahmat-Samii, "A single layer dual band circularly polarized microstrip antenna for GPS applications," *IEEE Antennas and Propagation Society International Symposium*, Vol. 4, pp. 720-723, June 2002.

- [4] Y. Lee, S. Ganguly, J. Yeo and R. Mittra, "A novel conformal multiband antenna design based on fractal concepts," *IEEE Antennas and Propagation Society International Symposium*, Vol. 1, pp. 92–95, June 2002.

- [5] Y. Lee, J. Yeo and R. Mittra, "A dual frequency circularly polarized antenna design using a combination of DRA and microstrip patch," *IEEE Antennas and Propagation Society International Symposium*, Vol. 4, pp. 122–125, June 2003.

- [6] D. M. Pozar, "Microstrip Antenna Aperture-Coupled to a Microstrip Line," *Electron. Lett.*, Vol. 21, pp.49-50, 1985.

- [7] Y. T. Lo, D. Solomon, W. F. Richards, "Theory and Experiment on Microstrip Antennas," *IEEE Trans. Antennas Propagat.*, Vol. AP-27, No.2, pp.137-145, March 1979.

- [8] L. C. Shen, S. A. Long, M. R. Allerdin, and M. D. Walton, "Resonant Frequency of a Circular Disk, Printed-Circuit Antenna," *IEEE Trans. Antennas Propagat.*, Vol. AP-25, No.4, pp.595-596, July 1977.

- [9] J. M. Tranquilla, J. P. Carr and H. M. Al-Rizzo, "Analysis of a Choke Ring Groundplane for Multipath Control in Global Positioning System (GPS) Applications," *IEEE Trans. Antennas Propagat.*, Vol. 42, No. 7, pp.905-911, July 1994.

- [10] M. Zhodzishsky, M. Vorobiev, A. Khvalkov, J. Ashjaee, "The First Dual-Depth Dual-Frequency Choke Ring," *Proc. Of ION GPS-98*, pp. 1035-1040, 1998.

- [11] Ansoft HFSS 8.0, www.ansoft.com

- [12] W. Kunysz, "High Performance GPS Pinwheel antenna," http://www.novatel.com/Documents/Papers/gps_pinwheel_ant.pdf

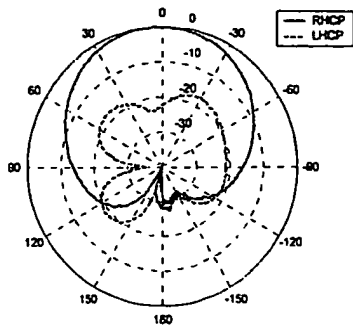


Figure 9. Measured RHCP and LHCP radiation patterns for tri-band GPS antenna at 1575MHz (L1)

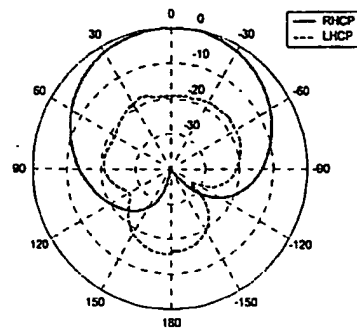


Figure 12. Measured RHCP and LHCP radiation patterns for Pinwheel™ antenna at 1227MHz (L2)

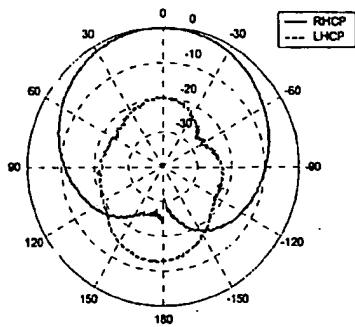


Figure 10. Measured RHCP and LHCP radiation patterns for tri-band GPS antenna at 1227MHz (L2)

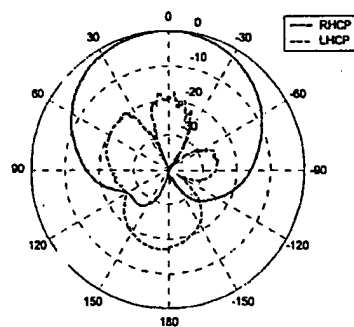


Figure 13. Measured RHCP and LHCP radiation patterns for Pinwheel™ antenna at 1575MHz (L1)

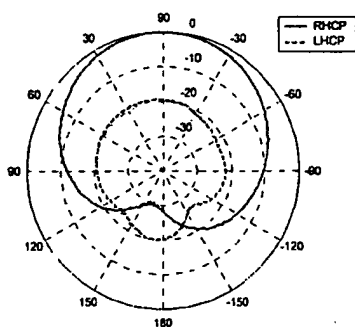


Figure 11. Measured RHCP and LHCP radiation patterns for tri-band GPS antenna at 1176MHz (L5)

Normalized to front RCP			Unit: dB		
	Pinwheel™		CRS Tri-band Antenna		
	L1	L2	L1	L2	L5
Front RCP	0	0	0	0	0
Back LCP	-20	-18	< -26.5	< -24	< -27
Back TOTAL	-20	-18	-26.5	-24	-27
Antenna diameter	203mm		198mm		

Table 2. Antenna pattern comparison

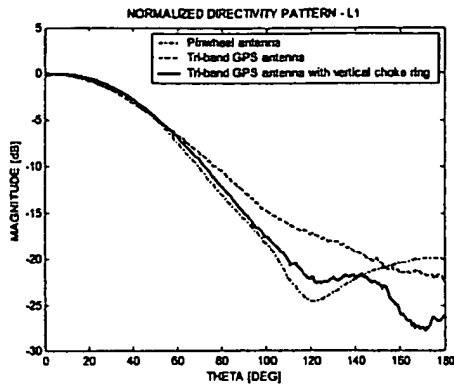


Figure 14. Total field pattern comparison at 1575MHz (L1)

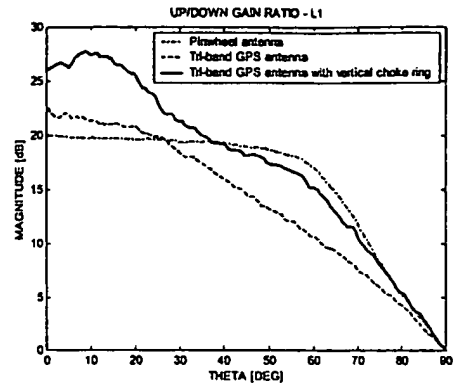


Figure 17. Up/Down Gain Ratio at 1575MHz (L1)

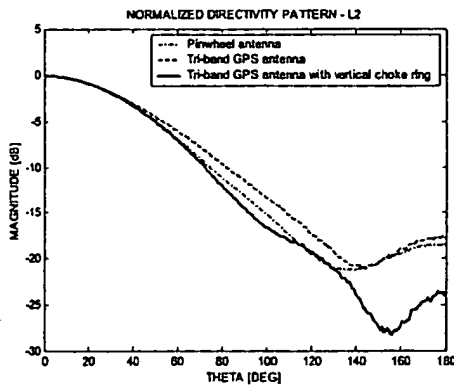


Figure 15. Total field pattern comparison at 1227MHz (L2)

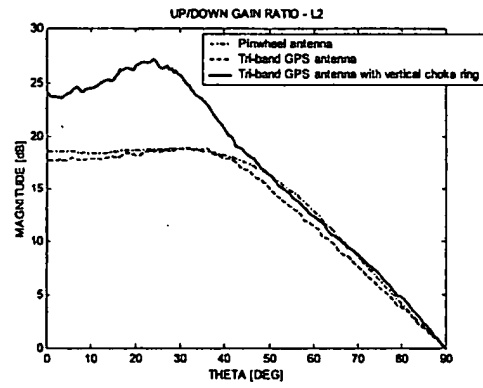


Figure 18. Up/Down Gain Ratio at 1575MHz (L2)

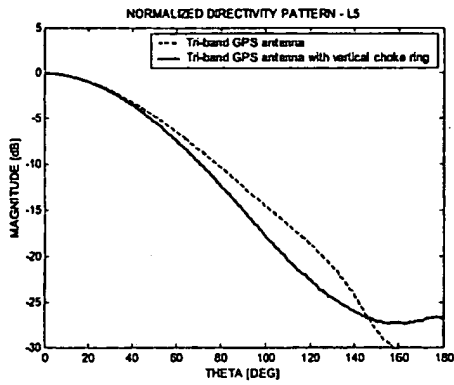


Figure 16. Total field pattern comparison at 1176MHz (L5)

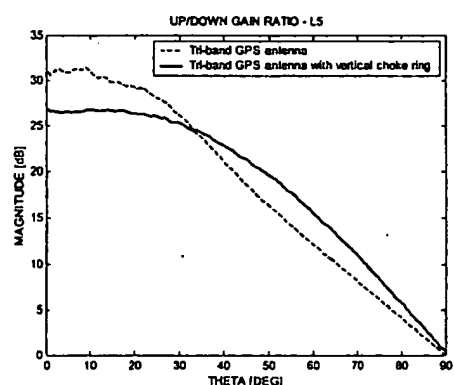


Figure 19. Up/Down Gain Ratio at 1575MHz (L5)